

Optical-Model Interpretation of Average Total Neutron Cross Sections in the keV Region*

A. P. JAIN, R. E. CHRIEN, J. A. MOORE, AND H. PALEVSKY

Brookhaven National Laboratory, Upton, New York

(Received 7 July 1964)

Total neutron cross sections for the elements Nb, Mo, Rh, Ag, Cd, and In in the range of 11 to 101 keV have been measured using the Brookhaven fast chopper at the NRU reactor, Chalk River, Canada. The data, after correction for sample thickness effects, are interpreted in terms of a spherical optical-model potential. The comparison of the data with the model indicates that the potential is more likely to be of the surface-absorption type rather than of the volume-absorption type. There is some evidence of fluctuations in S -wave strength functions from nuclide to nuclide, instead of the smooth variation predicted by the optical model. It seems that the parameters of the potential well, chiefly the imaginary part, may be different for S - and P -wave neutrons.

I. INTRODUCTION

THE optical model has been very successful in explaining the interaction of low-energy (S -wave) neutrons with nuclei.¹ The model predicts giant resonances in strength functions as a function of either mass number for a fixed neutron energy or as a function of energy for a fixed mass number. The strength function $\langle \Gamma_n^0 \rangle / D$ is defined as the average reduced neutron width $\langle \Gamma_n^0 \rangle$ divided by average level spacing D and is a measure of the absorption of the neutron wave in the nucleus. With the success of the model for S -wave neutrons,² many workers recently have evaluated the P -wave strength function from a measurement of capture^{3,4} and total cross sections^{5,6} in the kiloelectron volt region. The primary interest in the above measurements lies in measuring the strength of the spin-orbit potential in the model by observing the splitting of the P -wave giant resonance into $P_{3/2}$ and $P_{1/2}$ components. However, because of the dominance of the $l=0$ and $l=1$ partial waves in this energy region, one can also determine if the same parameters fit the S - and P -wave strength functions. Because of considerable disagreements in the results of Refs. 3 and 4, which constitute a major part of the published data, the total average cross sections of elements near $A \sim 100$ were measured from 10 to 100 keV of neutron energy using the Brookhaven fast chopper at the NRU reactor in Chalk River, Canada. The data are interpreted in terms of diffuse volume absorption and surface absorption optical model potentials.

II. EXPERIMENTAL METHOD

The BNL-AECL fast chopper facility⁷ was used for transmission measurements in the range of neutron energy 10 to 100 keV for the elements Nb, Mo, Rh, Ag, Cd, and In. These elements lie near the $3P$ giant resonance.¹

In the past, choppers have been used mainly in the low-energy region ($1 \lesssim$ keV); however, the P -wave contribution to the total cross section becomes big enough to be measured only above about 30 keV. With the best resolution available at the BNL-AECL facility, 15 nsec/m, it is easy to verify that for all the elements the resolution for energies greater than ~ 10 keV is so wide that only the average over Breit-Wigner levels (S and P) is obtained. This average cross section can then be interpreted in terms of the optical model. The chopper with its associated time-of-flight system, however, suffers from a background which is a function of the angular position of the rotor because of the transmission of fast neutrons and gamma-rays through the rotor. For accurate measurements (necessary to separate the small P -wave component from the total cross section) the knowledge of the chopper angle or the energy of the neutron for a fixed flight path at which this background becomes appreciable is very much desired. This can be done in a number of ways. In this experiment the transmission of a polyethylene sample $\frac{1}{4}$ in. thick, in the range of neutron energies from 10 to 100 keV, was measured. Polyethylene is mainly CH_2 . The cross section of CH_2 is mostly due to H_2 because of the small cross section of carbon relative to that of hydrogen. The energy at which the apparent cross section deviates from the expected cross section sets the upper limit for meaningful measurements in this experiment. At chopper angles less than this limit, the background becomes large. Hydrogen was chosen as a standard because it has the most accurately known cross section; it has no resonances and, therefore, no resolution effect, and finally it is the only cross section

* Work supported by the U. S. Atomic Energy Commission.

¹ H. Feshbach, C. E. Porter, and V. F. Weisskopf, *Phys. Rev.* **96**, 448 (1954).

² D. J. Hughes, R. L. Zimmerman, and R. E. Chrien, *Phys. Rev. Letters* **1**, 461 (1958).

³ L. W. Weston, K. K. Seth, E. G. Bilpuch, and H. W. Newson, *Ann. Phys.* **10**, 477 (1960).

⁴ J. H. Gibbons, R. L. Macklin, P. D. Miller, and J. H. Neiler, *Phys. Rev.* **122**, 192 (1961).

⁵ C. A. Uttley and R. H. Jones, *Proceedings of the Symposium on Neutron Time-of-Flight Methods, Saclay, France, 1961* (Euratom, Brussels, 1961), p. 109.

⁶ K. K. Seth, R. H. Tabony, E. G. Bilpuch, and H. W. Newson, *Bull. Am. Phys. Soc.* **8**, 120 (1963).

⁷ R. L. Zimmerman, H. Palevsky, R. E. Chrien, W. C. Olsen, P. P. Singh, and C. H. Westcott, *Nucl. Instr. Methods* **13**, 1 (1961).

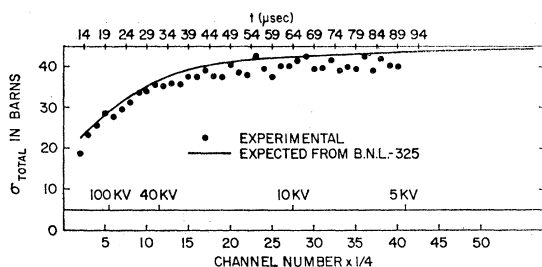


FIG. 1. The measured total cross section of CH_2 in the 100- to 5-keV range, shown by dots in the figure. The solid line is the curve from BNL 325.

that varies by a large amount between 100 keV and 2 to 3 MeV. The last point makes the hydrogen cross section the most sensitive for investigations of the transmission of the fast neutrons through the rotor. The effect for the heavier elements will be smaller because their average cross sections are not too different between 100 keV and 2 to 3 MeV.

Figure 1 shows the measured and expected cross section of CH_2 . The solid line is the expected curve from Ref. 8. The good agreement between the two for energies up to 100 keV gives confidence in our cross section measurements on heavier nuclei. The previously measured cross section of H_2 in 1 to 100 keV is also presently inaccurate to within a few percent and could be responsible for the small difference (2 to 3%) between the measured and expected cross sections.

The presence of rotor transmission background was also checked by comparing the measured cross sections of Cd and Ag with those measured previously⁸ by Van de Graaff groups. Good agreement between the two provides additional evidence that our measurements are good to within 2% or better.

In addition to the above-mentioned background there is another source, namely the overlap neutrons. At the top speed of 10 000 rpm, the overlap neutrons of about 72 eV from the previous burst arrive at the zero time of the next burst. This source of background was reduced to about $\frac{1}{2}\%$ of the beam intensity at 100 keV by putting a B^{10} filter (thickness 0.048 atoms/barn) at the exit stator of the chopper. The intensity in the 10 to 100 keV range was not appreciably reduced because of the $1/v$ cross section of B^{10} .

For absolute cross section measurements the sample in, sample out, and background runs were cycled every half hour to minimize systematic errors due to long-term variations in the signal and background rates recorded at the detector.

III. DATA ANALYSIS

In practice, a transmission measurement yields a sample transmission averaged over the resolution width of the spectrometer. However, the optical model pre-

dicts the average cross section. The two averages are the same for the thin samples, for which $T \approx 1 - n\sigma$. Here T is the transmission, σ the total cross section, and n the sample thickness. For practical transmission measurements, however, reasonably thick samples have to be used. The samples used in this experiment were such that $\langle T \rangle \sim 0.5$ for most of the samples. A sample thickness correction must be applied to the data. Because of the large Doppler broadening of the levels in the 10 to 100-keV range, the correction did not exceed a few percent for most of the elements.

The following procedure was used: The average (energy) transmission $\langle T \rangle$ can be written as

$$\begin{aligned} \langle T \rangle &= T_p(1 - \langle 1 - T_c \rangle) \\ &= T_p[1 - \langle (1 - T_c) / n\bar{\sigma}_c \rangle n\bar{\sigma}_c] \\ &= T_p(1 - I_c n\bar{\sigma}_c), \quad (1) \end{aligned}$$

where T_p is the transmission due to potential scattering, T_c and σ_c the transmission and cross section due to the compound nucleus part of the total cross section, n the sample thickness, and I_c the sample thickness correction factor. The $I_c = \langle 1 - T_c \rangle / n\bar{\sigma}_c$ can be easily calculated by averaging transmission and cross section over a single Breit-Wigner level, with some reasonable estimates of average level spacing and the radiation width.

The above is true only for a single isotope and one type of level. Most of the samples, however, have many isotopes. We have levels of up to two different spin states for the S -wave neutrons and four different spin states for the P -wave neutrons. Assuming that all these levels are uncorrelated the average transmission of the sample can be written as

$$\langle T \rangle = T_p \prod_i \langle T_i \rangle, \quad (2)$$

where the product is over all the different types of levels, S and P , from each isotope. The average of each of the factors on the right side of Eq. (2) is that given by (1) with n as the sample thickness of the particular isotope and I_c , the correction factor for a particular spin state. The corrections are computed assuming an average level only; no account was taken of the Porter-Thomas distribution of neutron widths.

For the evaluation of I_c for each of the terms in (2), we need Δ , Γ_γ , $\langle \Gamma_n^0 \rangle$, $\langle \Gamma_n^1 \rangle$, and R' ; where Δ is the Doppler width at the resonance energy, Γ_γ the radiation width, assumed to be the same for S and P waves, $\langle \Gamma_n^0 \rangle$ and $\langle \Gamma_n^1 \rangle$ are the average reduced neutron width for S and P wave neutrons, respectively, and R' the potential scattering radius. Δ depends on energy and atomic weight and can be easily evaluated at any energy E . Γ_γ is taken from Ref. 8 for each nucleus. For the evaluation of $\langle \Gamma_n^0 \rangle$ and $\langle \Gamma_n^1 \rangle$, the strength functions $\langle \Gamma_n^0 \rangle / D$ and $\langle \Gamma_n^1 \rangle / D$ are used together with the average level spacing D per spin state from BNL 325.⁸ The parameter D is assumed to be the same for S and P wave.

⁸ D. J. Hughes and R. B. Schwartz, Brookhaven National Laboratory Report No. BNL 325, 1958, 2nd. ed. (unpublished).

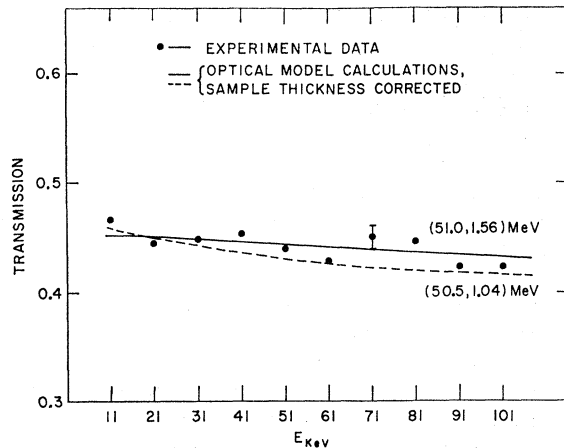


FIG. 2. The measured transmission of Cd shown by dots and the best fit curves based on the diffuse potential optical model calculations. The radius parameter is chosen to be $R = (1.15A^{1/3} + 0.4)F$ and the diffuseness parameter $a = 0.52F$. The real and the imaginary part, V_0 and W , respectively, of the potential is varied until a reasonable fit is obtained, after sample thickness correction is made. The calculated curves are labeled by values of V_0 and W , respectively.

For $\langle \Gamma_n^0 \rangle / D$ and $\langle \Gamma_n^1 \rangle / D$ and R' , an optical model calculation using a Saxon-Woods potential is performed for neutron energies from 1 to 101 keV at 10-keV energy intervals. The compound nucleus and shape elastic part of the calculation at 1 keV was then used to find $\langle \Gamma_n^0 \rangle / D$, $\langle \Gamma_n^1 \rangle / D$ and R' . The knowledge of R' is used in the evaluation of interference term in the Breit-Wigner formula. In the optical model calculation the radius R is assumed to be $R = (1.15A^{1/3} + 0.4)F$, and a , the diffuseness, to be $0.52F$. These are the parameters used by Campbell, Feshbach, Porter, and Weisskopf⁹ in their analysis of S -wave strength function data. The V_0 and W , the real and the imaginary parts of the potential, are varied until the average $\langle T \rangle$ [Eq. (2)], calculated as described above, agrees well with the measured transmission between 11 and 101 keV. Figure 2 shows such an agreement in a typical case of Cd. Two calculated curves are shown to indicate the sensitivity of the parameters to the measured transmission. This agreement is typical of those obtained for all the nuclei for which the measurements were made. The transmissions have a typical accuracy of 2% except in the case of Mo where they were a little higher, about 8%.

IV. INTERPRETATION

One method of interpretation is to use an extension of the procedure used by Hughes² and include the P -wave contribution to the total cross section. Such a procedure or its modification for the capture cross section has been

⁹ E. J. Campbell, H. Feshbach, C. E. Porter, and V. F. Weisskopf, Laboratory for Nuclear Science, MIT Technical Report No. 73, 1960 (unpublished).

used by Weston, Seth, Bilpuch, and Newson,³ Gibbons, Macklin, Miller, and Neiler⁴ in their interpretation of capture cross section, by Uttley and Jones,⁵ and Seth, Tabony, Bilpuch, and Newson⁶ in their interpretation of the total cross-section data. In this procedure, one obtains the strength functions for S and P wave from a least-squares fit to the data, using a linear relationship between strength function and cross section. These strength functions are then compared with different types of optical models. However, it has been shown (Ref. 10) that the use of linear approximation in the strength function, in the above procedure, is considerably inaccurate for energies greater than ~ 30 keV. The errors ($\sim 40\%$ or more) depend considerably on the maximum neutron energy and the element used and are difficult to predict. Because of the mixture of S and P waves in the measured cross section, this may affect the S and P -wave strength functions differently. For all these reasons it was decided to make a direct comparison of the measured cross sections with the optical model.

In this procedure one could still try to evaluate the strength functions. This was initially carried out at Brookhaven for the above-mentioned total cross section data. We first find the parameters (V_0, W) that best fit the data in the 11 to 101-keV range for each nucleus by computing the total neutron cross section from the optical model program as a function of energy from 11 to 101 keV. Then we use the following relations for the connection between the calculation of the compound nucleus cross section for S and P waves and the strength functions:

$$\sigma_e^{l=0}(1 \text{ keV}) = 13.0 \times 10^4 \langle \Gamma_n^0 \rangle / D$$

$$\sigma_e^{l=1}(1 \text{ keV}) = \frac{13.0 \times 10^4 \times 3k^2 R^2}{k^2 R^2 + 1} \left(\frac{\langle \Gamma_n^1 \rangle}{D} \right).$$

It is easy to check that the linear approximation is quite good at 1 keV. The potential used had no spin-orbit term included in it. The radius parameter r_0 and the diffuseness a of the well are kept the same for all the nuclei: $R = 1.25A^{1/3}F$ and $a = 0.52F$. Good fits, such as shown in Fig. 2, were obtained for all the nuclei between the neutron energy 11 to 101 keV. During the course of searching for the values of V_0 and W giving the best fit to the data, it was discovered that reasonable fits could be obtained for vastly different values of V_0 and W , corresponding to R_∞^1 of opposite sign.

Figure 3 shows the S and P -wave strength functions from an exhaustive search of the parameters V_0 and W , the other parameters being fixed at $R = 1.25A^{1/3}F$ and $a = 0.52F$. The two values of the P -wave strength functions for each nucleus correspond to two sets of values of V_0 and W . V_0 differs by about 4 MeV or so in the two cases and corresponds to positive and negative values of R_∞^1 , the P -wave distant-level parameter.¹⁰

¹⁰ A. P. Jain, Phys. Rev. **134**, B1 (1964).

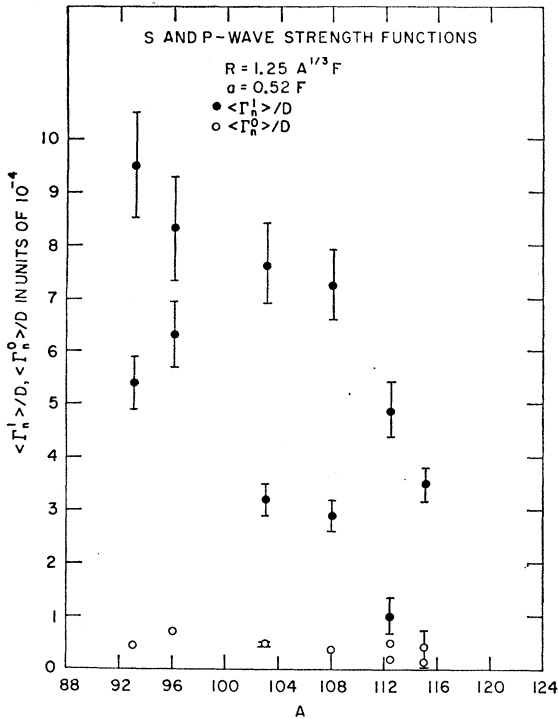


FIG. 3. *S*- and *P*-wave strength functions obtained from our data. The radius parameter R is chosen to behave as $R = 1.25A^{1/3}F$ for all the nuclei and the diffuseness parameter a to be $a = 0.52F$.

In addition, the *S*-wave hard-sphere radius $R' = R(1 - R_\infty^0)$, also differs in the two cases, for the same R , for each nucleus. The difference in a typical case of Nb^{93} is $\sim 9\%$. Therefore, effectively, we determine $\langle \Gamma_n^1 \rangle / D$, R_∞^1 , $\langle \Gamma_n^0 \rangle / D$, and R_∞^0 from such a procedure. There are two combinations of these parameters that fit the data; the *S*-wave strength functions $\langle \Gamma_n^0 \rangle / D$ are almost the same (within 10%) for the two cases. Similar results are obtained when r_0 in $R = r_0 A^{1/3}$, is changed to 1.35 instead of 1.25, used above. The *S*-wave strength functions so obtained agree well with the values quoted by Hughes, Zimmerman, and Chrien.

It should be emphasized that in Fig. 3 we have calculated V_0 and W independently for each nucleus. The V_0 and W so calculated are not necessarily then the same for each value of A . If we change the model, for example, to include the spin-orbit strength, or use the vibrational optical model of Buck,¹¹ then we get another set of values of the above quantities $\langle \Gamma_n^1 \rangle / D$, R_∞^1 , and R_∞^0 . Figure 4 shows the fit of the total cross section for Nb^{93} using three different sets of parameters, curves 1 and 2 with no spin-orbit potential and curve 3 with a spin-orbit potential of 8 MeV. Table I gives the values of $\langle \Gamma_n^1 \rangle / D$, $\langle \Gamma_n^0 \rangle / D$, R_∞^1 , and R_∞^0 for these three curves. For the case of curve 3, the values of R_∞^1 are not given. Because of the nonlinear behavior of the

¹¹ B. Buck and F. Perey, Phys. Rev. Letters 8, 444 (1962).

strength function relationship to cross section,¹⁰ it is not clear how to evaluate R_∞^1 from the cross section when the spin-orbit potential is present. Since the information about $\langle \Gamma_n^0 \rangle / D$ and $R' = R(1 - R_\infty^0)$ is presently not accurate enough to distinguish between any of these three cases, a different approach is adopted for subsequent analysis. In order to remove the ambiguity introduced by R_∞^1 , we chose the following procedure.

If the particular optical model chosen is good, then it should be possible to fit the total cross section as a function of energy for all the nuclei with the same set of parameters. Because of the limited energy range of the data, 11 to 101 keV, the test of the model is not complete until a fit is obtained for all the nuclides for the same parameters. Such a procedure suffers from the disadvantage that because of the large number of parameters in the model, it is difficult to obtain a unique set of parameters. In addition, many nuclear models are available today: volume absorption, surface absorption, or mixed volume and surface absorption, and spherical or vibrational models.¹¹ Furthermore, the parameters that fit the *S*-wave strength functions for $A \gg 100$ do not fit the data near $A = 100$.² Therefore there is no initial set of optical model parameters from

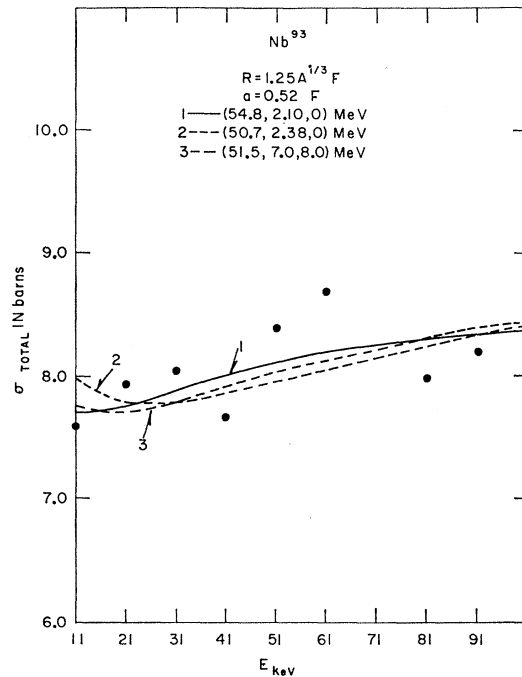


FIG. 4. The measured total cross section of Nb^{93} , corrected for sample thickness effects and the best fit optical model calculations. Curves 1 and 2 do not include any spin-orbit effects and curve 3 includes a spin-orbit coupling of 8 MeV. For curves 1 and 2, a volume absorption potential is used, the fixed parameters for which are $R = 1.25A^{1/3}F$ and $a = 0.52F$. For curve 3 a derivative type of surface absorption potential is used, with the width parameter $b = 0.40F$, other fixed parameters being the same as for curves 1 and 2. The curves are labeled by values of V_0 , W , and V_{s0} , respectively.

TABLE I. The values of $\langle \Gamma_n^0 \rangle / D$, R_{∞}^0 , $\langle \Gamma_n^1 \rangle / D$, and R_{∞}^1 for three values of potential parameters for which a good fit (see Fig. 5) to the measured total cross section of Nb⁹³ was obtained.

Curve No.	V_0 (MeV)	W (MeV)	V_{s0} (MeV)	$\langle \Gamma_n^0 \rangle / D \times 10^4$	R_{∞}^0	$\langle \Gamma_n^1 \rangle / D \times 10^4$	R_{∞}^1
1	54.8	2.10	0	0.519	-0.016	5.407	-0.824
2	50.7	2.38	0	0.500	-0.121	9.266	0.699
3	51.5	7.0	8.0	0.430	-0.096	6.72	...

which a start can be made. Nevertheless, the comparison is tried for the case of the spherical model.

For the spherical model, there are two commonly used shapes of the imaginary potential, volume absorption and surface absorption. As pointed out earlier,¹² the ratio of P - to S -wave strength functions for the same width of P -wave giant resonance is larger for the surface absorption than for the volume absorption model. Furthermore, the S -wave strength function near the P -wave giant resonance remains constant over a larger range of atomic weights for the surface absorption than for the volume absorption model. From Fig. 3, we notice that the experimental data for S -wave also shows the tendency of constancy over the entire range of measurements. For this reason a derivative type of

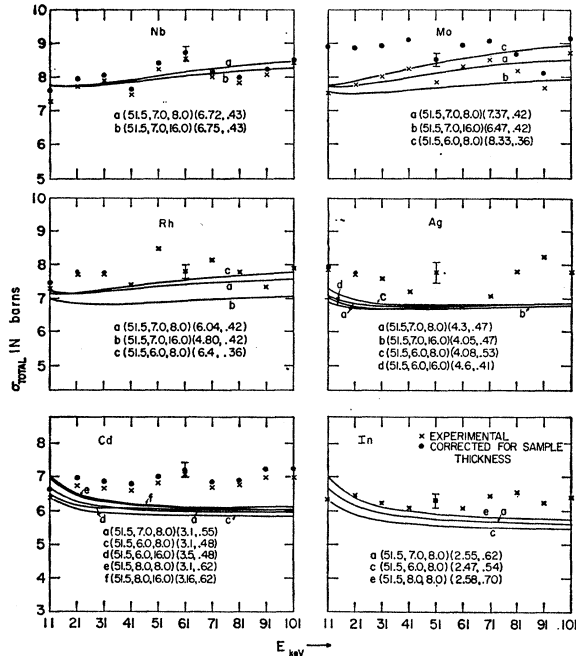


FIG. 5. Measured total cross section of Nb, Mo, Rh, Ag, Cd, and In, corrected for sample thickness effects and the optical model calculations with a derivative type surface absorption potential with fixed parameters the same as those of Fig. 4, curve 3. Each curve is labeled by two brackets. In the first bracket values of V_0 , W , and V_{s0} are listed, respectively, while in the second bracket the values of $\langle \Gamma_n^1 \rangle / D$ and $\langle \Gamma_n^0 \rangle / D$ are listed for the corresponding curve. The experimental points and the points corrected for finite sample thickness effects are shown in this figure and the two following it.

¹² A. P. Jain, Nucl. Phys. 50, 157 (1964).

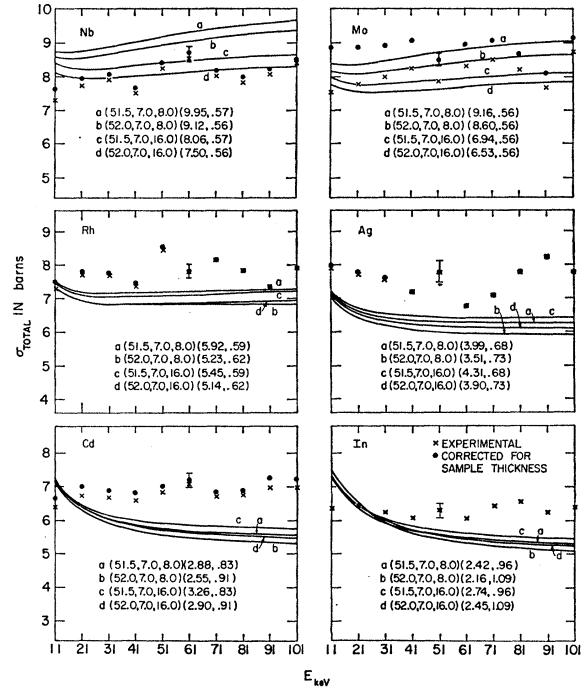


FIG. 6. The same data as in Fig. 5 and the optical model calculations. The fixed parameters, except a , were kept the same as in Fig. 5. The value of a was chosen to be $0.62F$ for all the curves.

surface absorption potential,

$$\frac{4W \exp[(r-R)/b]}{\{1 + \exp[(r-R)/b]\}^2},$$

is used for comparison with the data.

Figure 5 shows the data and the calculations. The r_0 in $R=r_0A^{1/3}$ was chosen to be $1.25F$, the diffuseness of the real part was chosen to be $0.52F$,⁹ and the width parameter b of the imaginary part to be $0.40F$. The real part of the potential V_0 was varied between 50 and 55 MeV, the imaginary part W , between 6 and 9 MeV, and the spin-orbit part V_{s0} between 8 and 16 MeV. The curves shown are the ones that came closest to the experimental data. Each curve is labeled by the quantities in two brackets. In the first bracket we list the values of V_0 , W , and V_{s0} , respectively, while in the second bracket we list the calculated P -wave and S -wave strength functions, respectively, for the corresponding curve, obtained from the 1-keV compound nucleus calculations of the same curve.

We notice that a reasonable fit is obtained for all the nuclei for the same potential parameters, $V_0=51.5$ MeV, $W=7$ MeV, and $V_{s0}=8$ MeV. In the worst cases Ag, Cd, and In, the disagreements are about 10%. This deviation is not unreasonable for an optical model calculation considering that the same set of parameters was used in fitting all the nuclides shown in Fig. 5. For example, the Cd fit shown in Fig. 2, although considerably better than shown in Fig. 5, proves to be

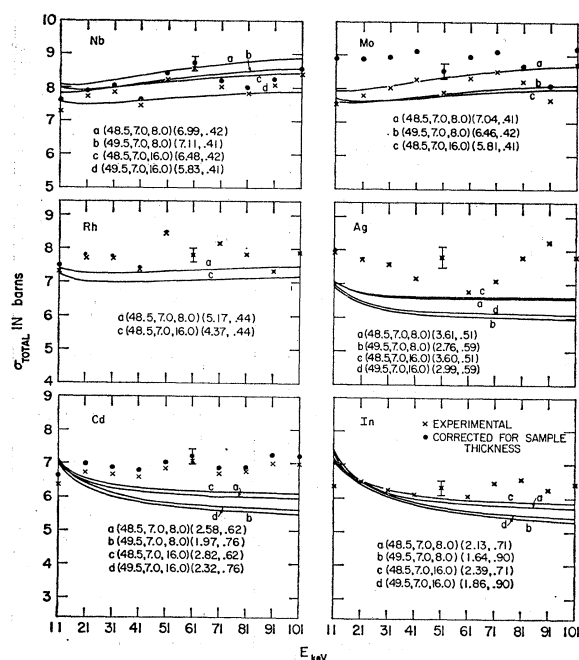


FIG. 7. The same data as in Fig. 5 and the optical model calculations with potential and parameters the same as in Fig. 5, except R , which is chosen to behave as $R=1.30A^{1/3}F$.

unrealistic when one tries to fit all the nuclides with the parameters used in Fig. 2.

Figure 6 shows the data and the calculations for the diffuseness $a=0.62F$. The other parameters are varied in the same way as above. Figure 7 shows the data and the calculations for $a=0.52F$, but r_0 changed to 1.30. In this case smaller values of V_0 are also included in the calculation to account for the increased r_0 .

V. DISCUSSION

The fits of Fig. 5 are a little better than those of Figs. 6 and 7, using as a basis of comparison a chi-square criterion. However, the agreement of the model to the data, for any one set of parameters is not very good in some nuclei, notably Ag, Cd, and In. There is small disagreement at the lower energy end even for Mo and Rh. However, such disagreements can be accounted for by small changes in the S -wave strength functions from those predicted by the model. The disagreements (Fig. 5) at the high-energy end for Cd and In can be accounted for by increasing the P -wave strength functions for these nuclei. This would mean that the P -wave giant resonance is wider than that predicted by a W of 7 or 8 MeV. This could be obtained by increasing the imaginary part of the potential, which, in turn, increases the S -wave part as well. In addition, increasing W decreases the value of the strength function in the neighborhood of the giant resonance peak. This decrease may be compensated by increasing the diffuseness a , which will further increase the S -wave strength function. A greater S -wave strength function will

result in a higher average total cross section below a neutron energy of 20 keV. A change in the radius parameter r_0 has little effect (see Fig. 7). Therefore, it seems that the S - and P -wave parameters needed to fit the data are different. Such a conclusion was also borne out by Krueger and Margolis¹³ in their interpretation of the data existing at that time.

One of the goals of the present work was to find the strength of the spin-orbit potential in the optical model. Weston, Seth, Bilpuch, and Newson,³ from a study of capture cross section data, found a large width for the $3P$ giant resonance, which was thought to be an evidence of large spin-orbit coupling. Our interpretation of their data would require a spin-orbit strength of about 16 MeV, in contrast to ≈ 8 MeV as obtained by Björklund and Fernbach¹⁴ from fits to high-energy neutron and proton scattering and polarization data. This is also shown to be the case by Krueger and Margolis¹³ in their interpretation of the previous data. The potential used by Krueger and Margolis is not, however, a conventional Saxon-Woods potential. In our case, it seems that the data demand a large imaginary potential, greater than 7 MeV, of the surface absorption type. The equivalent value for the volume absorption model is about 4 MeV. For such a value of W and a spin-orbit strength of 8 to 16 MeV, it is not possible to see a splitting of the $3P$ giant resonance by spin-orbit coupling. Because of this difficulty and that of differing parameters for S and P wave, it is difficult to distinguish between the two spin-orbit strengths, 8 or 16 MeV from our data. Our results show no evidence that the P -wave giant resonance is split, as has been suggested by Weston, Seth, Bilpuch, and Newson.³ The reason for this difference in interpretation may lie in the neglect of nonlinear terms in the capture cross sections in the simplified analysis of Weston *et al.* At present, it is not clear how to include the nonlinear terms in the analysis of capture cross section data.

For a better interpretation of the total cross section data, it is suggested that the total cross section be measured accurately from 0.5 to 10 keV. This cross section is primarily due to S wave. The S -wave contribution may then be extrapolated to the 11 to 101-keV range. Subtracting this from the present measured cross section in the same energy range the P -wave total cross section can be obtained. This cross section consists mainly of a P -wave compound nucleus cross section up to ~ 100 keV. The S - and P -wave components can then be separately compared with the model.

VI. CONCLUSIONS

From a fit of the total neutron cross section from 11 to 101 keV, with an optical model of the surface absorp-

¹³ T. K. Krueger and B. Margolis, Nucl. Phys. **28**, 578 (1961).

¹⁴ F. Björklund and S. Fernbach, Phys. Rev. **109**, 1295 (1958).

¹⁵ B. Block, H. Feshbach, and V. F. Weisskopf (private communication).

¹⁶ L. C. Gomes, Phys. Rev. **116**, 1226 (1959).

tion type, fair agreement is obtained. Detailed agreement, for all energies for which the measurements have been made, however, is not very good for all nuclides. There is some evidence of a fluctuation in the S -wave strength function for the nuclides investigated rather than the smooth values as a function of A expected from the optical model.

It also seems likely that the S - and P -wave parameters for the optical model may be different, and this could possibly account for the present lack of detailed agreement of the model with our data. More accurate measurements of the S -wave total neutron cross section in the low-energy range ($\lesssim 10$ keV) would be desirable as a check of this conclusion. The many-body calculation of Gomes for nuclear matter suggests that surface absorption should play a large part in forming the compound nucleus at low-incident neutron energies.

The better agreement of the present data with the surface absorption (rather than volume absorption) model supports this prediction. Because of the requirement of a large imaginary potential in interpreting our data, it is not possible to differentiate between spin-orbit strengths of 8 or 16 MeV. However, no potential within this range would show a splitting of the P -wave strength function near $A \cong 100$.

ACKNOWLEDGMENTS

The measurements reported in this paper were carried out at the NRU reactor in Chalk River, Canada, using the joint BNL-AECL fast chopper facility. We wish to thank our many colleagues at Chalk River for the help they provided in setting up this joint facility which made these measurements possible.

Prompt Neutrons from Thorium Photofission*

C. P. SARGENT, W. BERTOZZI, P. T. DEMOS, J. L. MATTHEWS, AND W. TURCHINETZ

Department of Physics and Laboratory for Nuclear Science, Massachusetts Institute of Technology, Cambridge, Massachusetts

(Received 27 March 1964; revised manuscript received 10 September 1964)

We have measured the distribution in angle and velocity of the prompt neutrons from the bremsstrahlung-induced photofission of Th^{232} in the photon energy region near threshold. Using knowledge of the fission-fragment angular distribution, the data have been interpreted in terms of the neutron distribution relative to the fragment axis. The measurement allows a quantitative estimate of the fraction of neutrons which are not emitted by fully accelerated fragments. The result for this fraction is 0.07 ± 0.09 . Assuming isotropic neutron emission in the fragment center-of-mass frame, the analysis also determines some characteristics of the neutron energy spectrum in this frame. The spectrum has an average energy $\bar{\eta} = 1.14 \pm 0.06$ MeV and a second central moment $\sigma^2(\eta) = (0.77 \pm 0.06)\bar{\eta}^2$. If it is represented by an evaporation-type spectrum with some distribution of temperatures, there is no significant contribution from temperatures equal to or greater than $\bar{\eta}$. We have made a similar analysis of data on prompt neutrons from the spontaneous fission of Cf^{252} obtained by Bowman, Thompson, Milton, and Swiatecki, and compared the results with those for Th^{232} photofission.

I. INTRODUCTION

THE recent rapid progress in the development of experimental techniques has provided a qualitative change in the experimental understanding of prompt-neutron emission in the fission process.¹⁻³ The most comprehensive prompt-neutron measurements reported to date are those of Bowman, Thompson, Milton, and Swiatecki,¹ in which neutrons from the spontaneous fission of Cf^{252} were measured in coincidence with the

fission fragments by a triple time-of-flight technique. Their results may be summarized as follows: (a) Most of the neutrons observed are emitted from fully accelerated fragments with an angular distribution which is isotropic in the center-of-mass frame of the moving fragment (henceforth abbreviated "c.m. frame"). (b) The shape of the energy distribution in the c.m. frame is independent of fragment mass A and kinetic energy E_k of the fission event, over a wide range of A and E_k . (c) Therefore, the prompt neutrons as observed (fragment charge, for example, is not observed) may be characterized by two functions of A and E_k , $\nu(A, E_k)$ and $\bar{\eta}(A, E_k)$, where ν is the number of neutrons emitted and $\bar{\eta}$ the average c.m. neutron energy. These functions have been determined for the Cf^{252} spontaneous-fission neutrons.¹ The strong A dependence of ν has been known

* This work is supported in part through funds provided by the U. S. Atomic Energy Commission under Contract AT(30-1)-2098.

¹ H. R. Bowman, S. G. Thompson, J. C. D. Milton, and W. J. Swiatecki, *Phys. Rev.* **126**, 2120 (1962); **129**, 2133 (1963). These references will be referred to as BTMS.

² S. S. Kapoor, R. Ramanna, and P. N. Rama Rao, *Phys. Rev.* **131**, 283 (1963).

³ K. Skarsvåg and K. Bergheim, *Nucl. Phys.* **45**, 72 (1963).